

# Formulation and Evaluation of Mouth Dissolving Film of Artemether and Lumefantrine by using Polymer

Umesh Deshta<sup>1\*</sup>, Bharat Khurana<sup>2</sup>

<sup>1</sup>\*Dept. of Pharmaceutical Sciences, AVIPS Shobhit University, Gangoh, Saharanpur, Uttar Pradesh, India, umesh.deshta@shobhituniversity.ac.in; umeshdeshta14@gmail.com, ORCID ID: <https://orcid.org/0009-0009-5038-7921>

<sup>2</sup>Dept. of Pharmaceutical Sciences, AVIPS Shobhit University, Gangoh, Saharanpur, Uttar Pradesh, India

---

## ABSTRACT

The fast-dissolving form of dosage has become a cutting-edge drug delivery method that lowers the frequency of administration while increasing therapeutic efficacy, bioavailability, and formulation stability. It allows for more effective systemic absorption by avoiding first-pass metabolism. This system speeds up the beginning of action by facilitating speedy drug absorption through the pre-gastric area. In the current study, artemether (ART) and lumefantrine (LMF) mouth dissolving film (MDF) formulations were prepared for the treatment and prevention of malaria. The solvent casting method was used to formulate the films, and their disintegration time, wetting time, percent drug release, and folding durability were assessed. The improved formulation showed good physicochemical properties, a high dissolution rate of  $81.0 \pm 1.00\%$  and a quick disintegration time of  $47.33 \pm 0.47$  seconds. These results suggest that the developed MDF is a potential and patient-friendly dosage form that can improve treatment compliance, speed up therapeutic effect, and improve drug delivery.

**Keywords:** Bioavailability, artemether (ART), lumefantrine (LMN), malaria, and mouth dissolving films (MDFs).

**How to cite this article:** Deshta U, Khurana B. Formulation and Evaluation of Mouth Dissolving Film of Artemether and Lumefantrine by using Polymer. *Int J Drug Deliv Technol.* 2026;16(23s): 219-244. DOI: 10.25258/ijddt.16.23s.25

**Source of support:** Nil

**Conflict of interest:** None

---

## INTRODUCTION

The world malaria report serves as the principal reference for global malaria burden assessment and policy orientation. It influences donor allocations and national strategic planning. The 2025 edition carries particular significance, arriving at a moment when the malaria control community confronts simultaneous challenges that collectively threaten the progress achieved since 2000.

The report's subtitle, "Addressing the threat of antimalarial drug resistance", signals a shift in perspective. For two decades, artemisinin partial resistance (ART-R) was characterized as a Southeast Asian problem requiring regional containment. This framing no longer holds. Resistance-associated mutations have emerged independently across eastern and southern Sub-Saharan Africa, transforming a distant concern into an immediate operational challenge.

This commentary examines the report's findings and their broader implications. The analysis suggests that the report, while comprehensive, may underestimate the systemic nature of the current threat. These threats differ in immediacy and severity. ART-R expansion, diagnostic

failure in the Horn of Africa, and acute funding disruption constitute immediate existential threats requiring urgent response. Artemisinin-based Combination Therapies (ACTs) partner drug efficacy decline and *An. stephensi* urban establishment represent medium-term threats that, if unaddressed, will compound current challenges within the coming decade. Underlying health system capacity gaps and surveillance infrastructure deficiencies represent structural vulnerabilities that amplify all other threats and constrain response options.

The 2025 report documents a tension between operational achievements and worsening aggregate indicators. Global malaria cases reached an estimated 282 million in 2024, with over 600,000 deaths, figures slightly higher than those recorded in 2023. These increases occurred predominantly in countries affected by conflict (Ethiopia, Yemen) or climatic disruption (Madagascar), illustrating how external shocks can rapidly erode programmatic gains.

Concurrent with these setbacks, the report documents substantive progress. Twenty-four countries have incorporated malaria vaccines into routine immunization programmes. Seasonal malaria chemoprevention reached

54 million children in 2024, compared with 0.2 million in 2012. Five countries attained malaria-free certification between 2024 and 2025. These achievements confirm that interventions remain effective when resources are sustained and health systems function adequately.

This pattern reveals a structural limitation. Current tools, insecticide-treated nets, antimalarial drugs, vaccines, are effective but insufficient to compensate for weak health systems or to absorb external shocks. Continued scale-up of existing interventions will yield diminishing returns unless underlying systemic vulnerabilities are addressed.

There has been growing interest in developing modified-release oral dosage forms, as oral drug delivery accounts for nearly 52% of the overall drug delivery market. However, several challenges are associated with oral administration, including the potential loss of active ingredients due to tablet or capsule crushing and inaccuracies in liquid dosing. These issues can result in imprecise dosing, leading to either drug overdosing or reduced therapeutic effectiveness. To address these challenges, fast-dissolving drug delivery systems have gained significant attention. Among these, oral film strips have become increasingly popular in recent years, originally introduced as a novel method for breath freshening. These thin, gel-like films are placed on the tongue, where they rapidly dissolve, releasing their flavour. Recent technological progress has prompted numerous pharmaceutical companies to investigate new possibilities in this field, aiming to achieve quick and precise dosing that can enhance patient compliance, especially in pediatric populations. Significant advancements have recently been made in transmucosal drug delivery routes, as this method offers effective solutions to many challenges linked to traditional oral drug administration. This dosage form eliminates the need for water or precise measurement, and once the film dissolves, the medication is easily swallowed. Drug absorption through the oral mucosa is particularly appealing because its rich vascularization ensures efficient permeability and rapid entry into systemic circulation. As a result, fast-dissolving films have gained popularity for delivering various medications, offering rapid disintegration due to their extensive surface area and ultimately enhancing patient compliance. Various hydrophilic polymers which provide rapid dissolution,

acceptable mechanical properties and good mouth feel quality are used as a film forming agents.

Hydroxypropyl methylcellulose (HPMC) is a semi-synthetic, cellulose-derived polymer composed of a cellulose backbone with hydroxypropyl and methyl substitutions. It is available in food and pharmaceutical grades and is widely utilized in various industries due to its excellent film-forming, thickening, and stabilizing properties. In the pharmaceutical industry, HPMC is used as a binder, coating agent, and controlled-release matrix, while in the food sector, it functions as a thickener, emulsifier, and stabilizer. HPMC exhibits good water solubility, film-forming ability, and biocompatibility, making it suitable for a broad spectrum of applications. Its ability to form heat-sealable films with good oxygen barrier properties also makes it a popular choice for packaging and protective coatings in food and pharmaceutical formulations.

Malaria is a severe mosquito-borne disease caused by *Plasmodium* parasites that infect human red blood cells. Artemether (ART) and lumefantrine (LMF) are effective antimalarial drugs commonly used in combination therapy to reduce the risk of infection and shorten the duration of illness. Artemether belongs to Biopharmaceutics Classification System (BCS) class II, whereas lumefantrine is categorized under BCS class IV. Both drugs possess distinct mechanisms of action that help minimize the development of parasite resistance. However, due to their poor water solubility, especially lumefantrine, the combination exhibits low dissolution rates and slow absorption, resulting in inadequate oral bioavailability. Dissolution studies and theoretical considerations suggest that reducing the particle size of these drugs enhances dissolution, thereby improving their solubility and overall oral bioavailability.

Hence, based on the rationale of the proposed research work, the aim of present investigation was to develop and formulate polymer-based mouth dissolving films of artemether (ART) and Lumefantrine (LMF) by solvent casting method for the direct absorption of drug via transmucosal lining to the systemic circulation. The proposed formulation has the potential to improve compliance and presents multiple competitive advantages over its marketed oral dosage forms used in prevention and treatment of malaria.

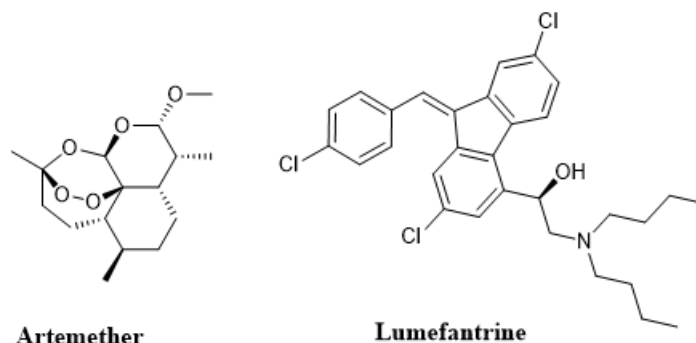


**Figure 1. Chemical structure of Artemether and Lumefantrine**

## 2. MATERIALS AND METHODS

### 2.1 Materials

The drug component Artemether (ART) and Lumefantrine (LMF) and excipients utilized for the preparation of mouth dissolving films of different compositions were obtained from authentic sources and authorized vendors while the drug artemether and lumefantrine was received as gift sample from Meridian Medicare Limited, HP, India. The ingredients used for formulations were of analytical grade and were utilized without any further purification.

### 2.2 Formulation development of fast dissolving films

#### 2.2.1 Preliminary trials for screening of components

The development of a successful fast dissolving film heavily depends on the nature and concentration of the

polymer used; various polymers were tested for their film-forming abilities. In the present study, hydroxy propyl methyl cellulose was selected as the film-forming polymer. Blank formulations were prepared by dissolving different polymers and plasticizer compositions in distilled water, as detailed in **Table 1 and Table 2**. The solutions were then cast and dried in an oven at 45 °C for 24 hours. The resulting films were evaluated for parameters such as surface appearance, stickiness, disintegration time, and folding endurance. HPMC is known for its excellent film-forming capacity, moisture retention, and oxygen barrier properties which contribute to the formation of uniform, flexible, and mechanically strong films suitable for mouth dissolving film applications.

**Table 1. Composition of blank mouth dissolving films by using HPMC E15**

Formulation ID#	HPMC (mg)	PEG400 (ml)	Water (ml)	Menthol (%)	Saccharin (%)	Ethanol (ml)
F1	200	5	15	1.0	0.3	3
F2	200	10	15	1.0	0.3	3
F3	300	5	15	1.0	0.3	3
F4	300	10	15	1.0	0.3	3
F5	400	5	15	1.0	0.3	3
F6	400	10	15	1.0	0.3	3
F7	500	5	15	1.0	0.3	3
F8	500	10	15	1.0	0.3	3
F9	600	5	15	1.0	0.3	3
F10	600	10	15	1.0	0.3	3

# Formulations containing variable amount of polymer.

**Table 2. Composition of blank mouth dissolving films by using EUDRAGIT L-100**

Formulation ID#	Eudragit L100 (mg)	PEG 400 (ml)	Dibutyl Phthalate (ml)	Triethyl Citrate (ml)	Acetone (ml)	Menthol (%)	Saccharin (%)
F1	200	5	-	-	5	1.0	0.3

F2	200	5	-	-	5	1.0	0.3
F3	300	5	-	-	5	1.0	0.3
F4	300	-	5	-	5	1.0	0.3
F5	400	-	5	-	5	1.0	0.3
F6	400	-	5	-	5	1.0	0.3
F7	500	-	-	5	5	1.0	0.3
F8	500	-	-	5	5	1.0	0.3
F9	600	-	-	5	5	1.0	0.3

# Formulations containing variable amount of polymer.

### 2.3 Preparation of drug loaded fast dissolving films

Polymeric solution (Solution A) was prepared by dissolving desired amount of hydroxy propyl methyl cellulose in sufficient quantity of distilled water (70%). Specific quantity of drug along with polyethylene glycol and other excipients were dissolved in remaining water (30%) with continuous stirring (Solution B). Solution B was slowly added in polymeric solution A with continuous stirring. Final solution obtained was kept

aside for 30 mins for defoaming. After defoaming, solution was poured in petri plate and dried at 45 °C in hot air oven for 24 h. Film casted in petri plate was then carefully peeled off and cut into pieces of desired shape and size. Different optimized combinations of film containing HPMC with PEG 400 were prepared as shown in **Table 3**. The prepared formulations were evaluated for the disintegration time, wetting time, folding endurance and percentage drug release.

**Table 3. Composition of oral mouth dissolving film of Artemether and Lumefantrine**

Formulation ID#	Artemether (mg)	Lumefantrine (mg)	HPMC (mg)	PEG 400 (ml)	Crospovi done (%)	Poloxamer 188 (%)	Water (ml)	Saccharin (%)	Menthol (%)	Ethanol (ml)
F1	20	120	200	5	1	0.5	15	0.3	1	3
F2	20	120	200	10	1	0.5	15	0.3	1	3
F3	20	120	300	5	1.5	0.5	15	0.3	1	3
F4	20	120	300	10	1.5	0.5	15	0.3	1	3
F5	20	120	400	5	2	1	15	0.3	1	3
F6	20	120	400	10	2	1	15	0.3	1	3
F7	20	120	500	5	2	1	15	0.3	1	3
F8	20	120	500	10	2	1	15	0.3	1	3
F9	20	120	600	5	3	1	15	0.3	1	3

# Formulations containing variable amount of polymer.

### 2.4 Evaluation of prepared aprepitant loaded MDF

#### 2.4.1 Drug excipient interaction study

##### 2.4.1.1 Fourier transform infrared spectroscopy (FTIR)

The Fourier Transform Infrared (FTIR) absorption spectra of the pure drug, hydroxypropyl methylcellulose (HPMC), and their physical mixture were obtained to analyze their molecular characteristics and interactions.

The spectra were recorded in the terms of the wavenumber range of 4000 to 400  $\text{cm}^{-1}$  using the potassium bromide (KBr) pressed pellet method. This method involved preparing samples by triturating a small amount of the substance (pure drug, HPMC, or their mixture) with KBr crystals, which is transparent to infrared radiation, and compressing the triturated mixture into a thin, transparent disc/pellet. The FTIR spectrophotometer (Spectrum GX, Perkin-Elmer, USA) was used to measure the infrared absorption, providing insights into the functional groups, chemical bonds, and potential interactions between the drug and HPMC in the mixture. The spectral range of 4000–400  $\text{cm}^{-1}$  covers key vibrational modes, including O-H, C-H, C=O, and other molecular stretching and bending vibrations, enabling detailed characterization of the samples.

#### **2.4.2 Thickness**

The thickness of each oral film was measured at five distinct locations to ensure a comprehensive assessment of uniformity and consistency across the film's surface. Measurements were conducted using a screw gauge, a precision instrument capable of accurately determining the thickness of thin materials. The screw gauge was carefully calibrated to ensure reliable and reproducible results. For each oral film formulation, the thickness values obtained from the five different points were recorded, and the average thickness was calculated to provide a representative value for the film. Additionally, the standard deviation of these measurements was computed to quantify the variability in thickness, indicating the degree of uniformity or potential irregularities in the structure of film.

#### **2.4.3 Weight variation**

To assess the weight uniformity of each oral film formulation, three film samples, each measuring  $2 \times 2 \text{ cm}^2$  ( $4 \text{ cm}^2$  in area), were randomly cut from different regions of the film to ensure representative sampling. The random selection of film sections helped account for potential variations in composition or thickness across the film surface. Each individual film sample was weighed using a high-precision electronic balance, which provided accurate and reliable measurements of mass. The weights of the three films from each formulation were recorded, and the mean weight for each formulation was calculated by averaging these values. This process allowed for the evaluation of weight consistency within and across formulations, which is critical for ensuring uniform drug content and quality in oral film formulations. The mean weight data served as an indicator of the films' physical uniformity, which is essential for their performance in applications in controlled drug delivery, as variations in weight could affect dosage accuracy and release profiles.

#### **2.4.4 Surface pH**

The surface pH of each oral film formulation was evaluated to assess its compatibility with the oral mucosa, as extreme pH values could cause irritation or discomfort during application. The test was conducted by placing an individual film sample in a clean Petri dish to provide a stable and controlled environment for measurement. The film was then moistened with 0.5 mL of phosphate buffer solution, which simulates the physiological conditions of the oral cavity and facilitates pH measurement. The buffer was allowed to interact with the film for 30 seconds to ensure adequate wetting of the surface. Subsequently, the electrode of a calibrated pH meter was brought into contact with the moistened surface of the film. To record accurate and stable readings, the pH meter was left in contact with the film for 1 minute, allowing sufficient time for equilibration of the electrode with the sample. To ensure reliability and account for potential variability, this procedure was repeated for three times for each film samples from individual formulation, and the average pH value was calculated from these values. This method provides a robust assessment of the surface pH, which is critical for confirming the safety and suitability of oral film formulations for mucosal administration.

#### **2.4.5 Folding endurance**

The folding endurance test was performed to evaluate the mechanical strength and flexibility of the oral film, specifically its ability to withstand repeated folding without breaking, which is an indicator of its tensile strength and durability. For this test, oral film samples with a uniform cross-sectional area and thickness were selected to ensure consistency and comparability of results. Each film was subjected to repeated folding at the same point, typically by bending it 180 degrees, until it either broke or developed visible cracks. The number of complete folds the film could endure before breaking was recorded as the folding endurance value. This value serves as a quantitative measure of the film's mechanical robustness, reflecting its ability to resist physical stress during handling, packaging, or application in the oral cavity. A higher folding endurance value indicates greater flexibility and tensile strength, which are critical for ensuring the film's integrity during manufacturing, storage, and use in drug delivery systems. This test is essential for confirming that the oral film can maintain its structural integrity under mechanical stress, thereby ensuring reliable performance in practical applications.

#### **2.4.6 Uniformity of drug content**

To determine the drug content uniformity across all oral film formulations, a random sampling approach was employed to ensure representative analysis. For each formulation, film samples measuring  $2 \times 2 \text{ cm}^2$  ( $4 \text{ cm}^2$  in area), referred to as the final dosage form (FDF), were randomly selected. Each selected film sample was dissolved in a phosphate buffer solution, chosen to mimic

physiological conditions and facilitate complete dissolution of the drug and excipients. The resulting solution was filtered to remove any insoluble residues or particulates, ensuring a clear sample suitable for analysis. The filtered solution was then analyzed using a UV-Visible spectrophotometer to quantify the drug content. The UV-Visible spectrophotometer method enabled precise detection of the drug based on its characteristic absorbance at a specific wavelength, providing an accurate measurement of its concentration. To ensure reliability and account for potential variability, the drug content analysis was performed in triplicate for each formulation, and the mean drug content was calculated from these three determinations. This approach ensured robust and reproducible results, verifying the uniformity and accuracy of drug loading in the oral film formulations, which is critical for ensuring consistent therapeutic efficacy and quality control in pharmaceutical applications.

#### 2.4.7 Percentage moisture loss

To evaluate the integrity and physical stability of the oral film formulation, a percent moisture loss test was conducted to assess the film's ability to retain or lose moisture under controlled conditions, which is critical for its stability during storage and handling. A film sample measuring  $2 \times 2 \text{ cm}^2$  ( $4 \text{ cm}^2$  in area) was carefully cut from each formulation to ensure uniformity in size and consistency. The initial weight of the film was measured using a high-precision electronic balance. Subsequently, the film was placed in a desiccator containing fused anhydrous calcium chloride, a highly effective desiccant that absorbs moisture, creating a low-humidity environment. The film was left in the desiccator for three days to allow sufficient time for any moisture present in the film to be removed. Further, the film patch was removed from the desiccator and weighed again using the same electronic balance to determine the final weight. The percentage moisture loss of the film was calculated using the following formula:

$$\text{Percentage Moisture Loss} = (\text{Initial Weight} - \text{final weight}) / \text{Initial Weight} \times 100$$

#### 2.4.8 In vitro wetting time

To assess the wetting time of the oral film formulation, which serves as an indicator of its hydrophilicity and ability to absorb moisture (an important factor for disintegration and drug release in the oral cavity), a standardized experimental procedure was employed. A circular piece of tissue paper, selected for its absorbent properties, was placed inside a clean Petri dish to create a uniform and controlled testing surface. A 6 mL solution of 0.1% w/v amaranth dye, a water-soluble red dye, was prepared and carefully added to the Petri dish, saturating the tissue paper. This dye solution was used to visually track the absorption process. A film strip, measuring  $2 \times 2$

$\text{cm}^2$  ( $4 \text{ cm}^2$  in area), was then gently placed on the surface of the dye-soaked tissue paper, ensuring consistent contact. The time taken for the amaranth dye to penetrate through the film and become visible on its upper surface was recorded as the wetting time. This duration reflects the film's ability to absorb the aqueous solution, indicating its potential behavior in the moist environment of the oral cavity. The wetting time is a critical parameter for evaluating the film's disintegration and dissolution properties, as faster wetting typically correlates with rapid drug release, which is desirable for oral film formulations in pharmaceutical applications. The experiment was conducted with precision to ensure reproducibility, and the use of amaranth dye provided a clear visual endpoint for accurate timing.

#### 2.4.9 Disintegration time

The disintegration time of the oral film formulation was determined to evaluate its ability to break down rapidly in a simulated physiological environment, a critical parameter for ensuring effective drug release in the oral cavity. A film strip measuring  $2 \times 2 \text{ cm}^2$  ( $4 \text{ cm}^2$  in area) was selected for its uniform size and consistency, ensuring reliable and comparable results. The film was placed in a Petri dish with a diameter of 6 cm, which provided a controlled and standardized testing environment. The Petri dish was filled with 6 mL of phosphate buffer solution maintained at a pH of 6.8, mimicking the pH of saliva in the oral cavity to simulate *in vivo* conditions. The time required for the film to completely disintegrate, defined as the point at which no solid residue of the film remained visible in the buffer, was carefully recorded using a stopwatch or timer. To ensure accuracy and account for potential variability, the disintegration test was performed in triplicate for each film formulation, with three separate film samples tested under identical conditions. The disintegration times from these three measurements were averaged to obtain a representative value, and the mean disintegration time was reported. This triplicate testing approach enhanced the reliability and reproducibility of the results, providing a robust assessment of the film's disintegration behavior, which is essential for optimizing its performance in oral drug delivery applications.

#### 2.4.10 In vitro release study

To evaluate the dissolution profile of the oral film formulations, an *in vitro* dissolution study was carried out to determine the rate and extent of drug release under conditions simulating the oral cavity environment. The study was performed using a beaker containing 30 mL of phosphate buffer (pH 6.8), which mimics the pH of human saliva and ensures physiological relevance. To enhance drug solubility and simulate the natural surfactants present in the oral cavity, 1% w/v sodium lauryl sulfate (SLS) was incorporated into the dissolution medium. The temperature of the medium was maintained

at  $37 \pm 0.5$  °C to replicate human body temperature. The entire setup, including the film and dissolution medium, was placed on a mechanical shaker to provide gentle agitation and ensure uniform drug release.

At predetermined time intervals, a 1.0 mL aliquot of the dissolution medium was withdrawn to monitor the progressive drug release. To maintain constant volume and sink conditions, each withdrawn sample was immediately replaced with an equal volume of fresh phosphate buffer (pH 6.8) containing 1% w/v SLS, pre-warmed to  $37 \pm 0.5$  °C. The samples were filtered to remove any undissolved film residues, ensuring clarity for spectrophotometric analysis. The filtered samples were suitably diluted with phosphate buffer (pH 6.8) to bring the concentration within the linearity range of the calibration curve.

Finally, the diluted samples were analyzed using a UV–Visible spectrophotometer at the drug's predetermined  $\lambda_{\text{max}}$  (260 nm), and the absorbance values were used to calculate the cumulative percentage drug release at each time point.

The *in vitro* release data obtained from the dissolution study were analyzed by fitting the data to three mathematical kinetic models—zero-order, first order, Higuchi, and Korsmeyer-Peppas models—to elucidate the drug release profile and underlying release mechanism. The zero-order model assumes a constant drug release

rate independent of the drug concentration, which is typical for controlled-release systems where the release rate remains steady over time. The Higuchi model describes drug release as a diffusion-controlled process, where the amount of drug released is proportional to the square root of time, commonly applicable to matrix-based systems like oral films. The Korsmeyer-Peppas model, a semi-empirical model, was used to further characterize the release mechanism by analyzing the release exponent ( $n$ ), which indicates whether the release is governed by Fickian diffusion ( $n \leq 0.45$ ), non-Fickian (anomalous) transport ( $0.45 < n < 0.89$ ), or case-II transport ( $n \geq 0.89$ ), such as polymer swelling or erosion. By fitting the dissolution data to these models, the release kinetics and mechanisms were determined, providing critical insights into whether the drug release was driven by diffusion, matrix erosion, or a combination of these processes. This comprehensive analysis was essential for understanding the performance of the oral film formulation, optimizing its design, and ensuring its suitability for effective and controlled drug delivery in oral applications.

### 3. RESULTS

#### 3.1 Characterization of artemether and lumefantrine loaded fast dissolving films

##### 3.1.1 Organoleptic properties

The organoleptic features of the drug were observed, and the observations were recorded in **Table 4**.

**Table 4. Organoleptic properties of artemether and lumefantrine**

Sr. No	Property	Inferences (Artemether)	Inferences (Lumefantrine)
1.	Color	White colored buff powder	Yellow Powder
2.	Taste	Bitter	Bitter
3.	Odor	Odorless	Odorless
4.	Melting point	86 to 88°C	130 to 132 °C
5.	Solubility	Sparingly soluble in water Soluble in, acetone, methanol, and ethanol. Insoluble in methylene chloride	sparingly soluble in aqueous buffers
6.	Physical form	Crystalline	Amorphous

##### 3.1.2 Identification of drug

###### 3.1.2.1 Determination of absorption maxima of Artemether

Determination of absorption maxima of the prepared solution (10, 20, 30, 40, 50, 6, 70, 80, 90, 100, 110, 120

µg/mL) of Artemether in methanol was scanned individually on a double beam UV spectrophotometer, and the absorption maxima were observed at 260 nm.

**Table 5. Determination of absorption**

Con.(µg/ml)	Absorbance 1	Absorbance 2	Absorbance 3	Mean Abs <sup>[a]</sup>
10	0.065	0.052	0.074	0.064±0.011
20	0.095	0.1	0.109	0.101±0.007
30	0.135	0.142	0.154	0.144±0.010
40	0.171	0.187	0.199	0.186±0.014

50	0.234	0.24	0.257	0.244±0.012
60	0.274	0.28	0.297	0.284±0.012
70	0.323	0.329	0.346	0.333±0.012
80	0.374	0.38	0.397	0.384±0.012
90	0.427	0.423	0.433	0.424±0.008
100	0.457	0.466	0.483	0.469±0.013
110	0.5	0.502	0.519	0.507±0.010
120	0.539	0.545	0.562	0.549±0.012

[a] Mean±SD of absorbance of three different experiments.

### 3.1.2.2 Determination of absorption maxima of Lumefantrine

Determination of absorption maxima of the prepared solution (10, 20, 30, 40, 50, 60, 70, 80, 90, 100, 110, 120

µg/mL) of Lumefantrine in methanol was scanned individually on a double beam UV spectrophotometer, and the absorption maxima were observed at 234 nm.

Table 6. Determination of absorption

Con.(µg/ml)	Absorbance 1	Absorbance 2	Absorbance 3	Mean Abs <sup>[a]</sup>
10	0.071	0.068	0.075	0.071 ± 0.004
20	0.118	0.122	0.129	0.123 ± 0.006
30	0.168	0.172	0.179	0.173 ± 0.006
40	0.216	0.221	0.228	0.222 ± 0.006
50	0.265	0.271	0.279	0.272 ± 0.007
60	0.315	0.321	0.328	0.321 ± 0.007
70	0.364	0.369	0.377	0.370 ± 0.007
80	0.413	0.419	0.427	0.420 ± 0.007
90	0.462	0.468	0.475	0.468 ± 0.007
100	0.511	0.517	0.525	0.518 ± 0.007
110	0.560	0.566	0.573	0.566 ± 0.007
120	0.608	0.614	0.622	0.615 ± 0.007

[a] Mean±SD of absorbance of three different experiments.

### 3.1.2.3 Development of calibration curve

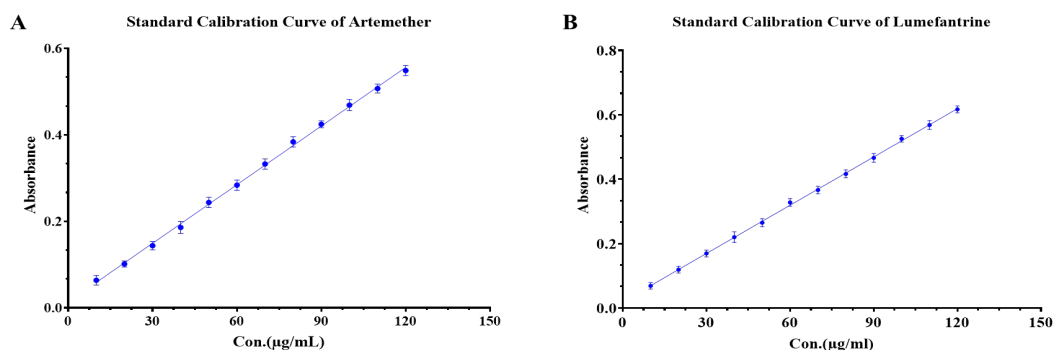


Figure 2. Standard calibration of drug a) Artemether and b) Lumefantrine

### 3.2 FTIR spectral analysis

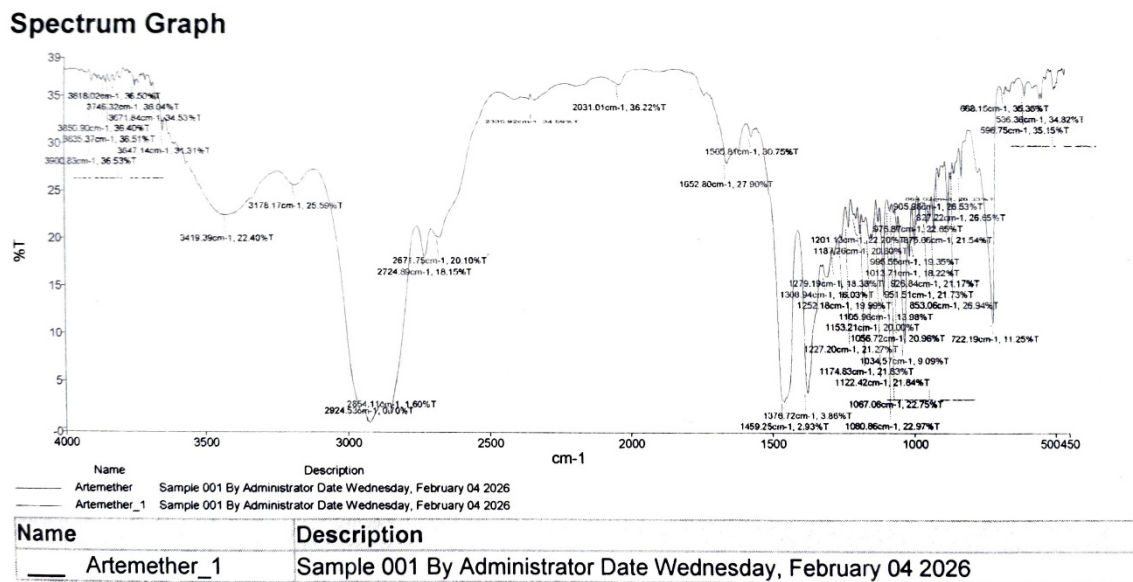


Figure 3. FTIR Spectroscopy graph of artemether

A broad absorption band observed in the range 3419–3818  $\text{cm}^{-1}$  corresponds to O–H stretching vibrations, attributable to hydroxyl functionalities and intermolecular hydrogen bonding. Prominent peaks between 2924–3178  $\text{cm}^{-1}$  are assigned to aliphatic C–H stretching vibrations of  $\text{CH}_2$  and  $\text{CH}_3$  groups. Weak bands in the 2671–2724  $\text{cm}^{-1}$  region may be due to overtone or combination vibrations.

A distinct absorption at  $\sim 1652 \text{ cm}^{-1}$  confirms the presence of the lactone carbonyl ( $\text{C}=\text{O}$ ) group. The band at  $\sim 1505 \text{ cm}^{-1}$  represents skeletal C–C stretching vibrations. The fingerprint region (1000–1250  $\text{cm}^{-1}$ ) shows intense C–O–C stretching, indicative of ether and peroxide linkages, while the endoperoxide (O–O) stretch is expected near  $\sim 880 \text{ cm}^{-1}$ . These features collectively confirm the structural integrity of artemether (Figure 3).

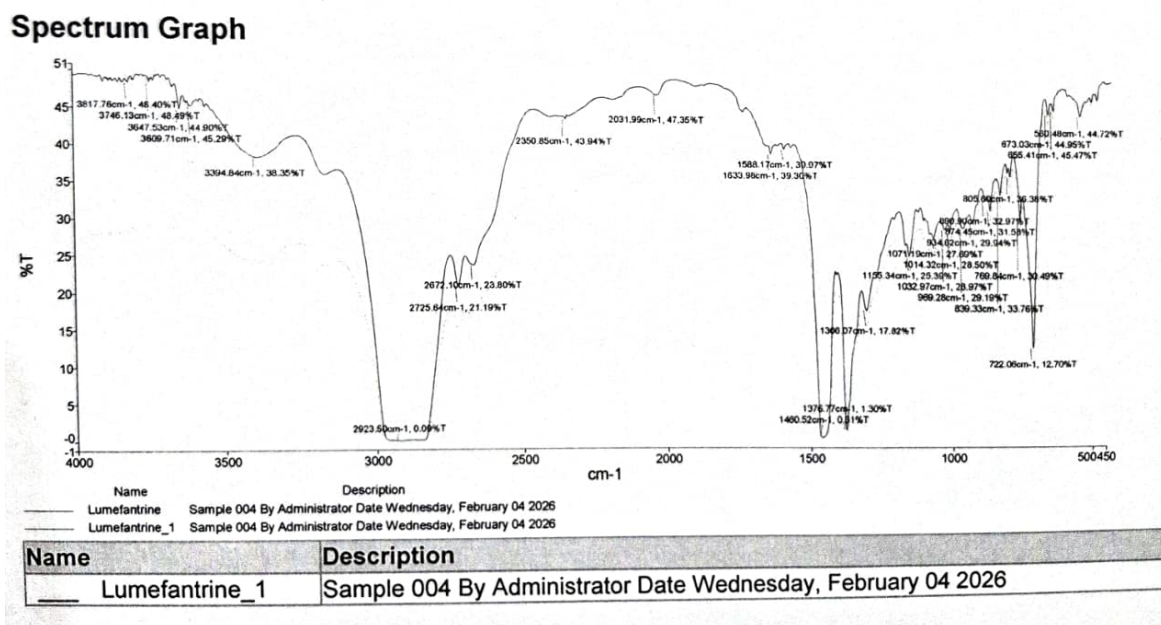


Figure 4. FTIR Spectroscopy graph of Lumefantrine

Broad bands in the region 3817–3647  $\text{cm}^{-1}$  are attributed to O–H and N–H stretching vibrations. A strong absorption at  $\sim 2923 \text{ cm}^{-1}$  corresponds to aliphatic C–H stretching of the long alkyl chain. Peaks in the 2672–2725  $\text{cm}^{-1}$  region may arise from protonated amine groups or overtone bands.

The aromatic framework is confirmed by strong absorptions in the 1588–1633  $\text{cm}^{-1}$  range due to C=C

stretching vibrations of the naphthalene and phenyl rings. Bands at 1460–1376  $\text{cm}^{-1}$  correspond to C–H bending and C–N stretching. The 1032–1071  $\text{cm}^{-1}$  region indicates C–O stretching of the secondary alcohol group. A prominent band at  $\sim 722 \text{ cm}^{-1}$  represents aromatic C–H out-of-plane bending, characteristic of substituted chlorinated aromatic rings (**Figure 4**).

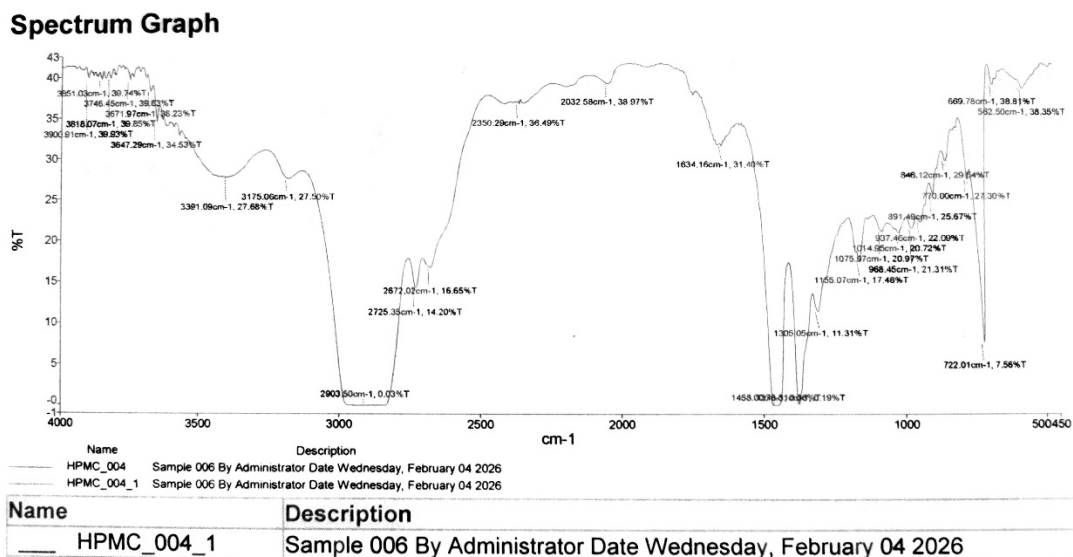
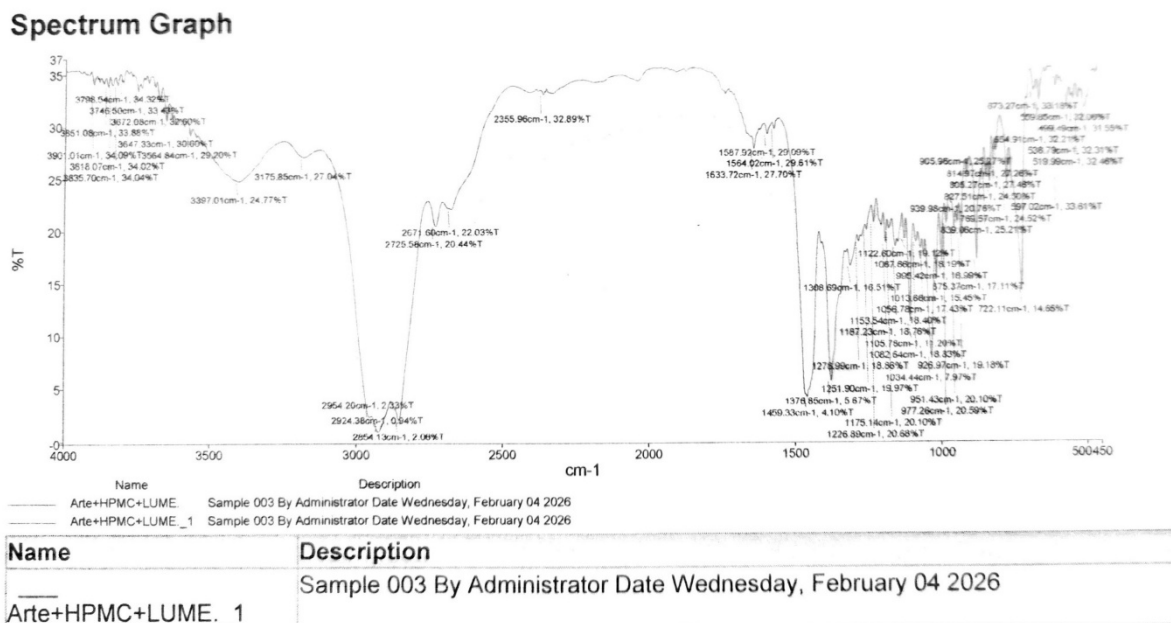


Figure 5. FTIR Spectroscopy graph of HPMC

A very broad and intense band in the range 3651–3900  $\text{cm}^{-1}$  corresponds to O–H stretching due to extensive hydrogen bonding within the polymer matrix. Peaks between 2903–2725  $\text{cm}^{-1}$  are assigned to aliphatic C–H stretching vibrations. The band at  $\sim 1634 \text{ cm}^{-1}$  is attributed to O–H bending of absorbed moisture.

The most diagnostic feature is the strong absorption in the 1155–1075  $\text{cm}^{-1}$  region, corresponding to C–O–C stretching of glycosidic linkages. Additional peaks in the 891–966  $\text{cm}^{-1}$  region arise from pyranose ring vibrations, while the band at  $\sim 722 \text{ cm}^{-1}$  is associated with skeletal vibrations of the cellulose backbone (**Figure 5**).



**Figure 6. FTIR Spectroscopy graph of Artemether and Lumefantrine**

The FTIR spectrum of the combined formulation represents the most informative profile, indicating the presence of a physical mixture or co-processed blend of artemether, lumefantrine, and hydroxypropyl methylcellulose (HPMC). A broad absorption band observed in the range of 3387–3788  $\text{cm}^{-1}$  corresponds to O–H stretching vibrations, arising from the hydroxyl groups of HPMC along with contributions from lumefantrine. The region between 2671–2964  $\text{cm}^{-1}$  exhibits characteristic C–H stretching vibrations, confirming the presence of aliphatic moieties contributed by all three components.

Distinct absorption bands in the range of 1567–1633  $\text{cm}^{-1}$  are attributed to aromatic C=C stretching vibrations, confirming the retention of lumefantrine's aromatic structure within the formulation. The fingerprint region (800–1300  $\text{cm}^{-1}$ ) displays a complex, composite pattern resulting from the overlap of characteristic peaks of all components, including C–O–C stretching vibrations of

HPMC, ether and peroxide linkages of artemether, and aromatic out-of-plane bending vibrations of lumefantrine.

Importantly, no significant peak shifts, disappearance of characteristic bands, or emergence of new peaks were observed in the formulation spectrum. This indicates the absence of chemical interactions among the components, thereby confirming that the drugs and polymer are physically compatible and maintain their structural integrity within the formulation.

Overall, the overlay of the combination spectrum with the individual components suggests the formulation blend retains the characteristic functional groups of all ingredients without evidence of new covalent interactions, which is a positive indicator for pharmaceutical compatibility studies (Figure 6).

### 3.3 Evaluation parameters for placebo MDF

Evaluation parameters of placebo oral dispersible film were observed and the observation were recorded in Table 8.

**Table 8. Evaluation parameter of Blank MDF**

Formulation ID#	Wt. Variation <sup>[a]</sup>	Thickness <sup>[b]</sup>	Folding endurance <sup>[c]</sup>	Disintegration Time <sup>[d]</sup>	Surface pH <sup>[e]</sup>
F1	21.05±0.10	0.22±0.09	51±2	43±2	6.70±0.03
F2	18.95±0.11	0.16±0.07	56±1	45±2	6.71±0.03
F3	18.02±0.14	0.17±0.08	63±2	42±2	6.74±0.02
F4	18.90±0.20	0.13±0.05	81±2	38±3	6.78±0.01

F5	21.10±0.30	0.14±0.06	91±3	36±2	6.79±0.02
F6	16.95±0.18	0.13±0.03	55±2	41±1	6.72±0.01
F7	21.00±0.15	0.15±0.02	57±2	41±2	6.73±0.02
F8	18.95±0.22	0.16±0.06	66±2	40±2	6.76±0.02
F9	17.90±0.12	0.14±0.04	68±3	44±2	6.75±0.02

[a] = percent weight; [b] = millimeter; [c] = unitless; [d] = Time in seconds; data are shown as mean±SD of 3 different experiments; # Blank formulations containing variable amount of polymer.

### 3.4 Formulation of mouth dissolving film

Mouth dissolving film of Artemether and Lumefantrine was prepared by Solvent Casting Method. The mouth dissolving film of Artemether and Lumefantrine was shown in **Figure 7**.



**Figure 7. Final optimized MDF of artemether and lumefantrine by solvent casting method**

### 3.5 Evaluation parameters for MDF of Artemether and lumefantrine

Evaluation parameters of oral dispersible film of Artemether and Lumefantrine were observed and the observations presented into following sections.

#### 3.5.1 Evaluation of weight variation of MDF of Artemether and Lumefantrine

The % weight variation data for nine polymer-containing formulations (F1–F9) of the combination mouth

dissolving film of Artemether and Lumefantrine (showed mean values ranging from 23.78% (F3) to 27.16% (F9), indicating the impact of increased total drug load along with varying polymer concentrations on weight uniformity. Formulation F4 exhibited the highest reproducibility (SD = 0.64%), demonstrating better formulation consistency, whereas F5 and F6 showed relatively higher variability (SD = 1.48% and 1.51%, respectively), suggesting possible formulation-related inconsistencies or uneven drug-polymer distribution.

**Table 9. Weight variation evaluation of MDF of Artemether and Lumefantrine**

Formulation ID <sup>#</sup>	% wt. variation			Mean <sup>[a]</sup>
	Experiment 1	Experiment 2	Experiment 3	
F1	24.18	26.12	27.05	25.78±1.45
F2	23.05	24.10	24.86	24.00±0.90
F3	23.89	22.35	25.10	23.78±1.39
F4	24.20	24.75	25.48	24.81±0.64
F5	23.95	25.92	26.88	25.58±1.48

F6	25.80	22.84	24.96	24.53±1.51
F7	23.70	22.96	24.85	23.84±0.96
F8	26.10	24.68	23.92	24.90±1.10
F9	26.32	27.05	28.10	27.16±0.89

[a] Mean±SD of three different experiments; # formulations containing variable amount of polymer.

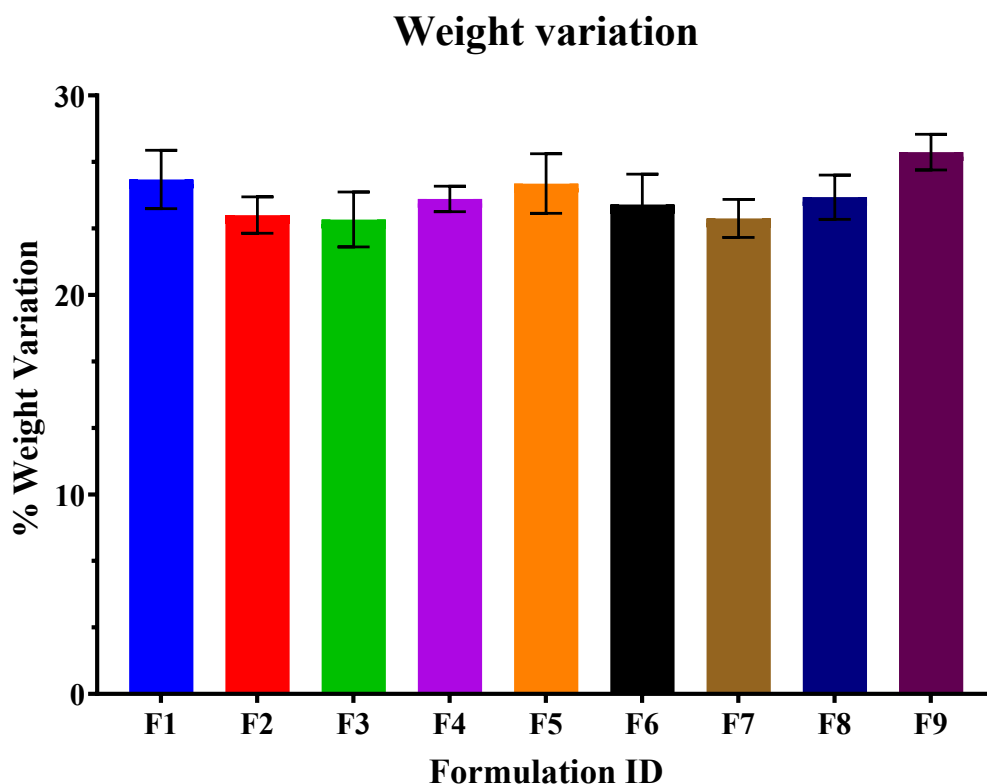


Figure 8. Graphical presentation of weight variation of all formulations (F1–F9).

### 3.5.2 Thickness evaluation of MDF of Artemether and Lumefantrine

The thickness of Artemether–Lumefantrine mouth dissolving films (F1–F9) ranged from 0.19 mm (F8) to 0.26 mm (F3, F6), reflecting increased drug loading and polymer content. Most formulations showed high

reproducibility ( $\pm 0.01$  mm), while F2 and F8 had slightly higher variability ( $\pm 0.02$  mm). Formulations F3–F7 demonstrated uniform thickness and are suitable for optimization, whereas F2 and F8 may require further refinement.

Table 10. Thickness evaluation of MDF of Artemether and Lumefantrine

Formulation ID <sup>#</sup>	Thickness <sup>[a]</sup>			Mean <sup>[b]</sup>
	Experiment 1	Experiment 2	Experiment 3	
F1	0.22	0.21	0.23	0.22±0.01
F2	0.23	0.22	0.20	0.22±0.02

F3	0.25	0.26	0.27	0.26±0.01
F4	0.21	0.22	0.22	0.22±0.01
F5	0.20	0.21	0.19	0.20±0.01
F6	0.26	0.25	0.27	0.26±0.01
F7	0.20	0.22	0.21	0.21±0.01
F8	0.18	0.19	0.21	0.19±0.02
F9	0.21	0.23	0.22	0.22±0.01

# formulations containing variable amount of polymer; [a] = thickness in millimetre; [b] = mean±SD of 3 different experiments.

### Thickness of formulations

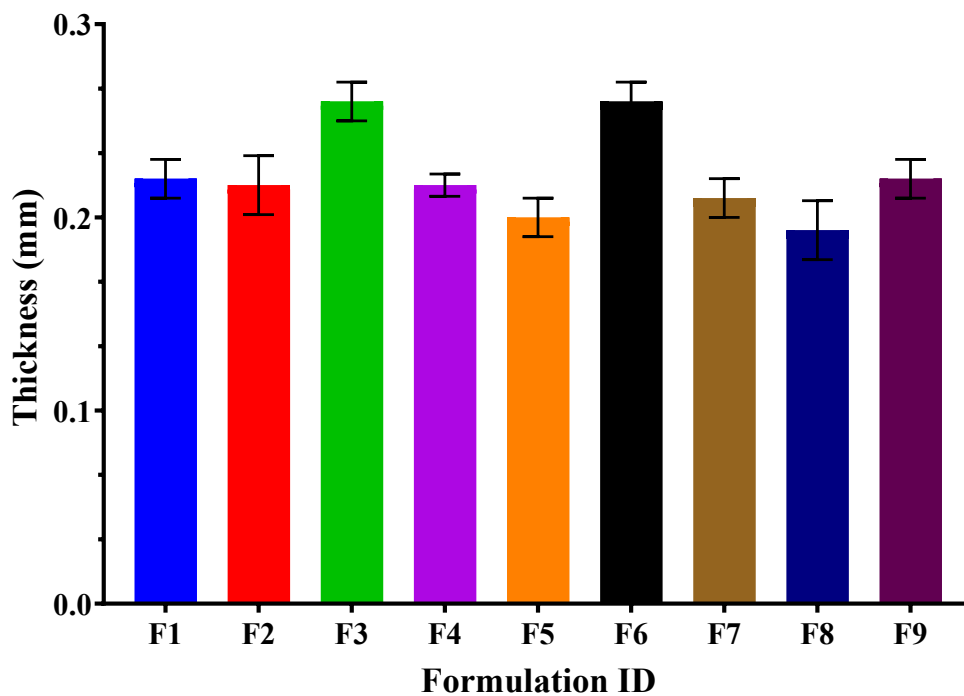


Figure 9. Comparative analysis of thickness of mouth dissolving films formulations (F1-F9)

#### 3.5.3 Percent moisture loss evaluation of MDF of Artemether and Lumefantrine

The % moisture loss of Artemether–Lumefantrine mouth dissolving films (F1–F9) ranged from 4.17% (F4) to 6.00% (F3), reflecting the effect of drug loading and polymer composition on moisture retention. F4 and F1

showed lower moisture loss, indicating better stability, while F3 and F8 exhibited higher loss. Most formulations showed acceptable reproducibility, though F8 had slightly higher variability. Overall, F1 and F4 are more suitable for stable formulations, whereas F6 and F8 require further optimization.

Table 11. Percent moisture loss evaluation of MDF of Artemether and Lumefantrine

Formulation ID <sup>#</sup>	% Moisture loss <sup>[a]</sup>			Mean <sup>[b]</sup>
	Experiment 1	Experiment 2	Experiment 3	
F1	4.2	4.3	4.4	4.30±0.10

F2	5.6	5.5	5.7	5.60±0.08
F3	5.9	6.0	6.1	6.00±0.10
F4	4.0	4.2	4.3	4.17±0.15
F5	4.5	4.8	4.7	4.67±0.15
F6	5.4	5.2	5.1	5.23±0.15
F7	5.8	5.6	5.5	5.63±0.15
F8	6.0	5.8	5.6	5.80±0.20
F9	4.9	4.7	4.6	4.73±0.15

# formulations containing variable amount of polymer; [a] = percent moisture loss; [b] = mean±SD of 3 different experiments.

### Percent moisture loss in formulations

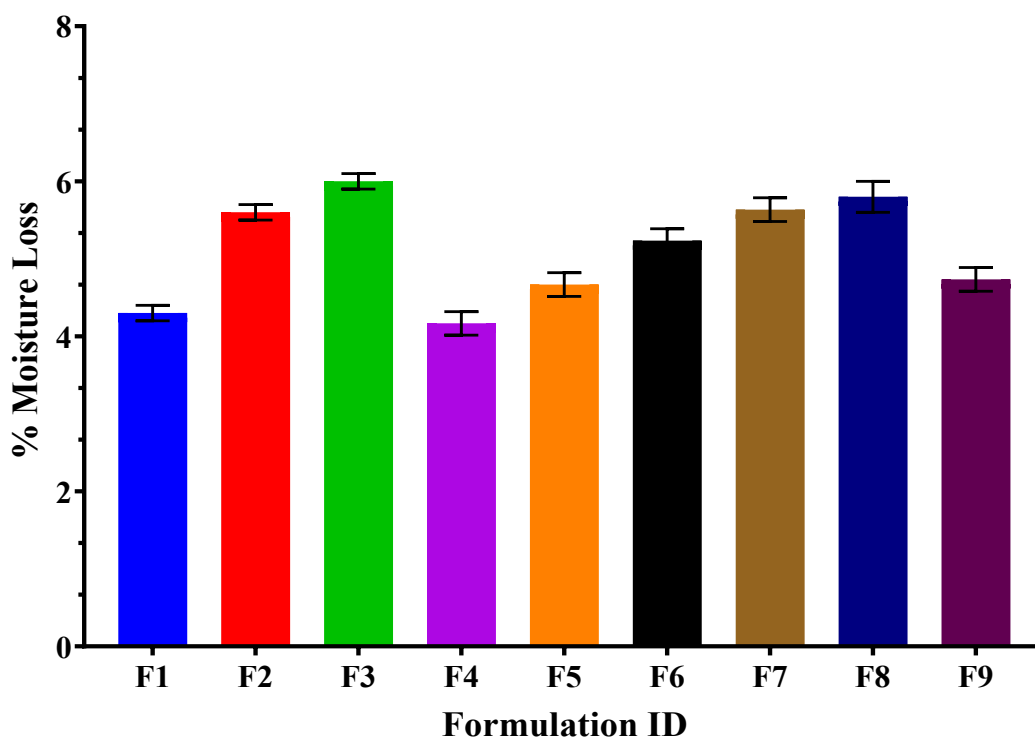


Figure 10. Comparative analysis of % moisture loss of mouth dissolving films formulations (F1-F9)

#### 3.5.4 Folding endurance evaluation of MDF of Artemether and Lumefantrine

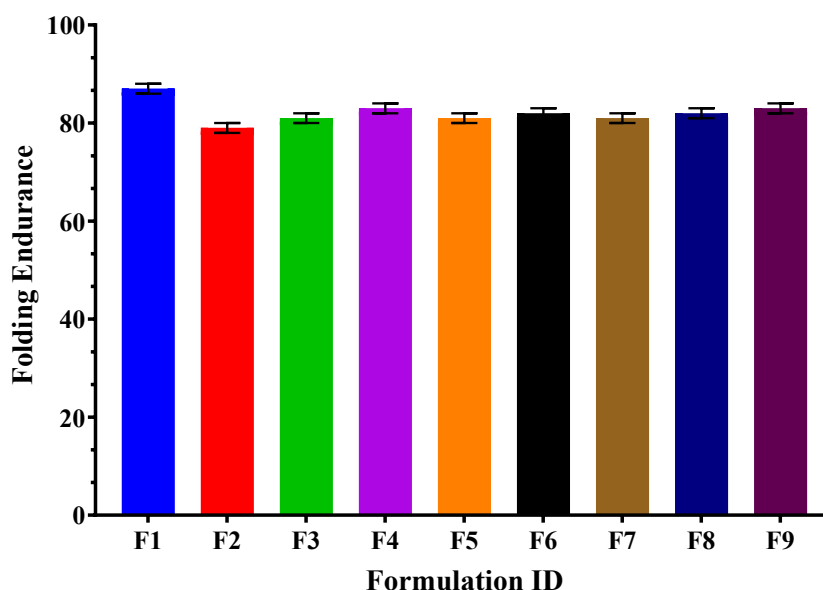
The folding endurance of formulations (F1–F9) of the Artemether and Lumefantrine mouth dissolving film ranged from 79.00 (F2) to 87.00 (F1), indicating variation in mechanical strength due to polymer composition and

drug loading. F1 showed the highest flexibility, while F2 exhibited the lowest durability. Most formulations (F3–F9) displayed similar endurance (81.00–83.00) with consistent reproducibility ( $\pm 1.00$  SD). Overall, F1 is optimal for flexibility, whereas F2 requires further optimization to enhance mechanical strength.

**Table 12. Folding endurance evaluation of MDF of Artemether and Lumefantrine**

Formulation ID <sup>#</sup>	Folding endurance <sup>[a]</sup>			Mean <sup>[b]</sup>
	Experiment 1	Experiment 2	Experiment 3	
F1	88	86	87	87.00±1.00
F2	78	80	79	79.00±1.00
F3	82	81	80	81.00±1.00
F4	83	82	84	83.00±1.00
F5	82	81	80	81.00±1.00
F6	83	81	82	82.00±1.00
F7	82	80	81	81.00±1.00
F8	83	82	81	82.00±1.00
F9	84	82	83	83.00±1.00

# formulations containing variable amount of polymer; [a] = thickness in millimetre; [b] = mean±SD of 3 different experiments.

**Folding endurance of formulations****Figure 11. Comparative analysis of folding endurance of mouth dissolving films formulations (F1-F9)**

### 3.5.5 Wetting time evaluation of MDF of Artemether and Lumefantrine

The wetting time of Artemether–Lumefantrine mouth dissolving films (F1–F9) ranged from 15.00 sec (F4) to 28.33 sec (F2), indicating the effect of polymer composition on hydration. F4 showed the fastest and

most consistent wetting, suitable for rapid release, while F2 showed the slowest. F3 and F5 also exhibited faster wetting, whereas F7–F9 showed slower and more variable performance. Overall, F4 is optimal, while F2, F7, and F9 require further optimization.

**Table 13. Wetting time evaluation of MDF of Artemether and Lumefantrine**

Formulation ID <sup>#</sup>	Wetting Time <sup>[a]</sup>			Mean <sup>[b]</sup>
	Experiment 1	Experiment 2	Experiment 3	
F1	18	17	19	18.00±1.00
F2	28	27	30	28.33±1.53
F3	17	16	18	17.00±1.00
F4	15	14	16	15.00±1.00
F5	16	17	19	17.33±1.53
F6	19	20	22	20.33±1.53
F7	25	26	23	24.67±1.53
F8	18	20	23	20.33±2.52
F9	25	27	24	25.33±1.53

# formulations containing variable amount of polymer; [a] = wetting time in seconds; [b] = mean±SD of 3 different experiments.

### Wetting time of formulations

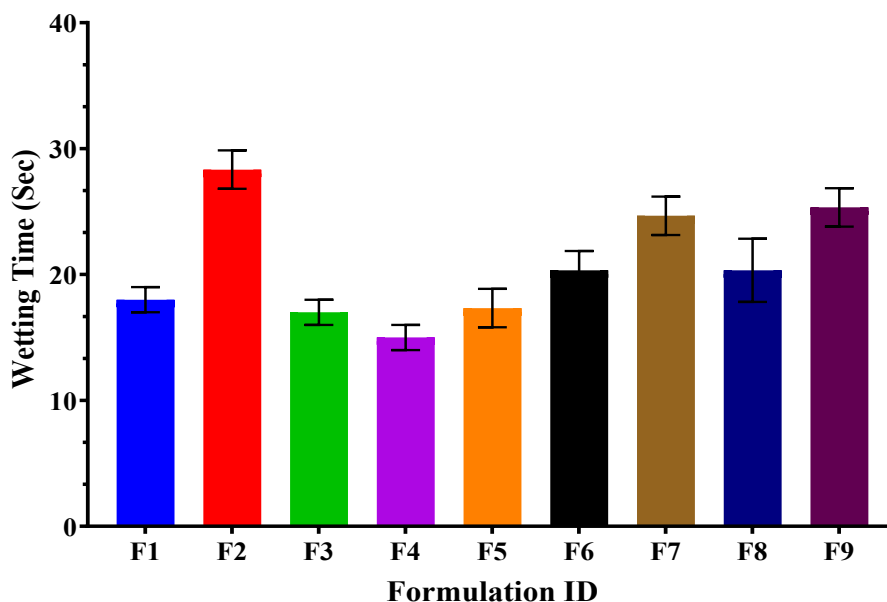


**Figure 12. Comparative analysis of wetting time of mouth dissolving films formulations (F1-F9)**

### 3.5.6 Disintegration time evaluation of MDF of Artemether and Lumefantrine

The disintegration time of the prepared mouth dissolving films (F1–F9) ranged from 47.33 seconds (F4) to 58.00 seconds (F2), demonstrating the influence of polymer concentration and film-forming characteristics on the rate

of film disintegration in simulated oral conditions. Formulations F4 and F8 exhibited relatively faster disintegration ( $47.33 \pm 0.47$  and  $49.00 \pm 0.82$  seconds), which may be attributed to the formation of thin, less dense, and more porous films, allowing rapid penetration of saliva and quick film hydration.

**Table 14. Disintegration time evaluation of MDF of Artemether and Lumefantrine**

Formulation ID <sup>#</sup>	Disintegration Time <sup>[a]</sup>			Mean <sup>[b]</sup>
	Experiment 1	Experiment 2	Experiment 3	
F1	52	51	52	51.67 ± 0.47
F2	59	57	58	58.00 ± 0.82
F3	50	51	50	50.33 ± 0.47
F4	47	48	47	47.33 ± 0.47
F5	53	52	51	52.00 ± 0.82
F6	49	50	51	50.00 ± 0.82
F7	58	57	56	57.00 ± 0.82
F8	48	49	50	49.00 ± 0.82
F9	57	56	55	56.00 ± 0.82

# formulations containing variable amount of polymer; [a] = disintegration time in seconds; [b] = mean±SD of 3 different experiments.

### Disintegration Time of formulations

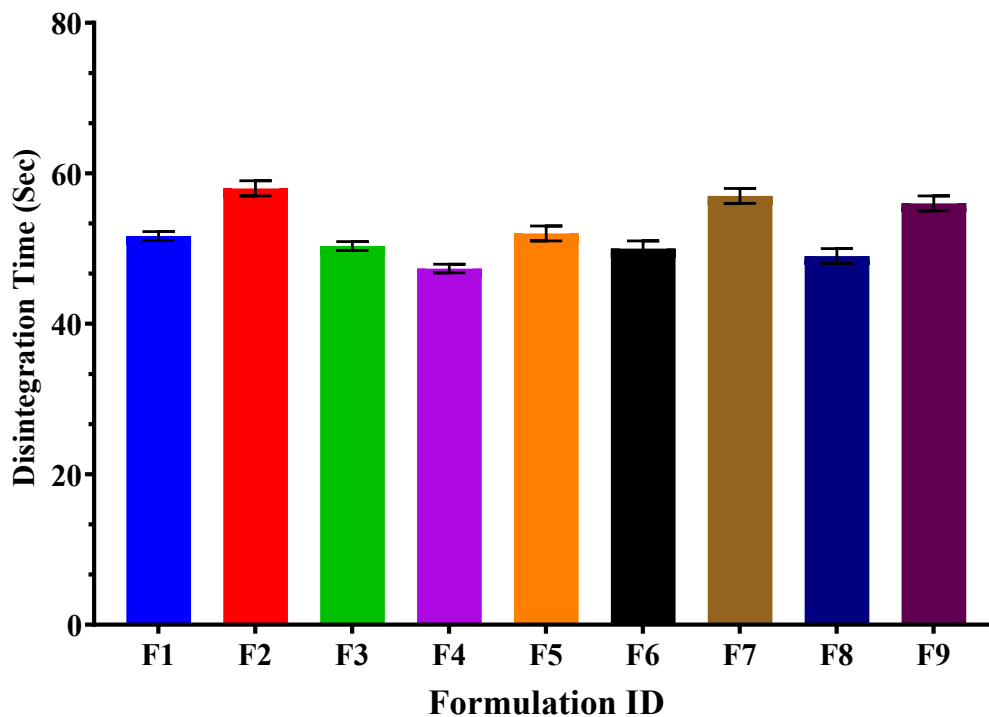


**Figure 13. Comparative analysis of disintegration time of mouth dissolving films formulations (F1-F9)**

### 3.5.7 Surface pH evaluation of MDF of Artemether and Lumefantrine

The surface pH of Artemether–Lumefantrine mouth dissolving films (F1–F9) ranged from 6.68 (F4) to 6.81 (F5), remaining within the near-neutral physiological range, indicating suitability for oral use. Most formulations (F1, F2, F6, F7, F8) showed high

consistency ( $SD \approx 0.01$ ), while F4 and F9 exhibited slightly higher variability ( $SD \approx 0.02$ ). The narrow pH range suggests minimal influence of polymer variation, with F5 showing slightly higher and F4 slightly lower pH. Overall, all formulations are acceptable, though F4 and F9 may require minor optimization.

*Table 15. Surface pH evaluation of MDF of Artemether and Lumefantrine*

Formulation ID <sup>#</sup>	Surface pH			Mean <sup>[a]</sup>
	Experiment 1	Experiment 2	Experiment 3	
F1	6.72	6.69	6.71	6.71 ± 0.01
F2	6.75	6.73	6.76	6.75 ± 0.01
F3	6.78	6.75	6.77	6.77 ± 0.01
F4	6.68	6.67	6.70	6.68 ± 0.02
F5	6.81	6.79	6.82	6.81 ± 0.01
F6	6.76	6.74	6.73	6.74 ± 0.01
F7	6.77	6.75	6.74	6.75 ± 0.01
F8	6.80	6.78	6.77	6.78 ± 0.01
F9	6.79	6.77	6.75	6.77 ± 0.02

# formulations containing variable amount of polymer; [a] = mean±SD of 3 different experiments.

### Surface pH of formulations

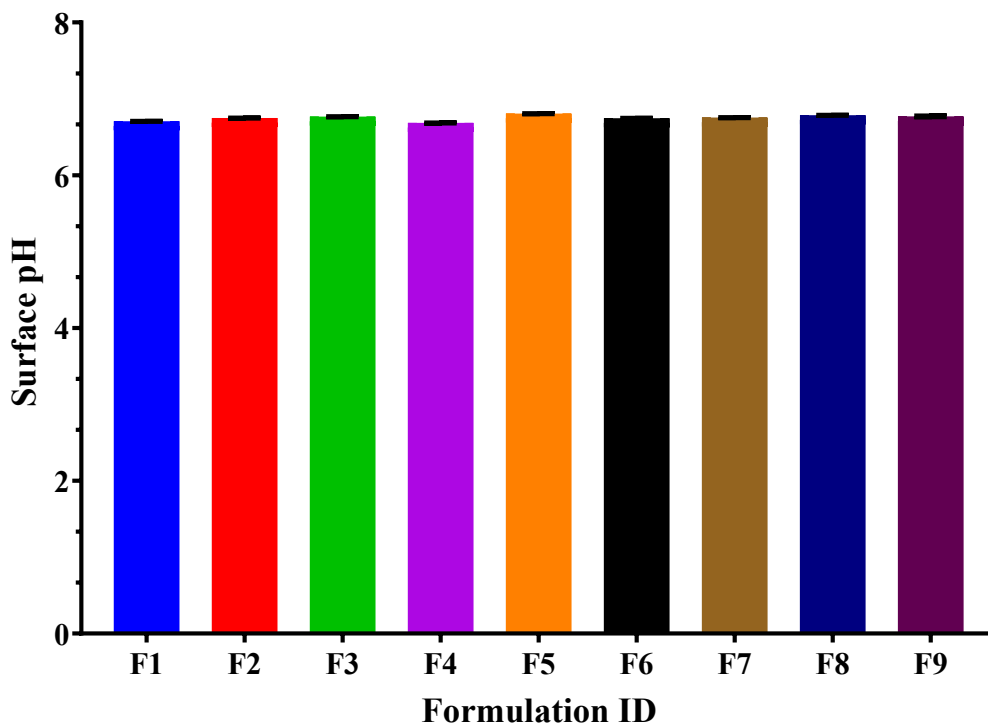


Figure 14. Comparative analysis of surface pH of mouth dissolving films formulations (F1-F9)

#### 3.5.8 Percent drug release evaluation of MDF of Artemether and Lumefantrine

The percent drug release of Artemether–Lumefantrine mouth dissolving films (F1–F9) ranged from 73% (F7) to 83% (F4), with F4 showing the highest release and good consistency. Most formulations exhibited acceptable

uniformity, though F2 and F5 showed slightly higher variability. F4 demonstrated an optimal balance of high drug release and consistency, making it a promising formulation, while F7 showed the lowest release. Overall, F1, F3, and F5 also exhibited satisfactory release but may require minor optimization for better consistency.

Table 16. Percent drug release evaluation of MDF of Artemether and Lumefantrine

Formulation ID <sup>#</sup>	Percent drug release			Mean <sup>[a]</sup>
	Experiment 1	Experiment 2	Experiment 3	
F1	78	80	82	80 ± 1.63
F2	74	77	80	77 ± 2.45
F3	79	82	78	80 ± 1.70
F4	81	83	80	81 ± 1.53
F5	79	77	82	79 ± 2.05
F6	78	76	75	76 ± 1.25
F7	72	75	73	73 ± 1.25
F8	77	75	78	77 ± 1.25
F9	76	77	74	76 ± 1.25

# formulations containing variable amount of polymer; [a] = mean±SD of 3 different experiments.

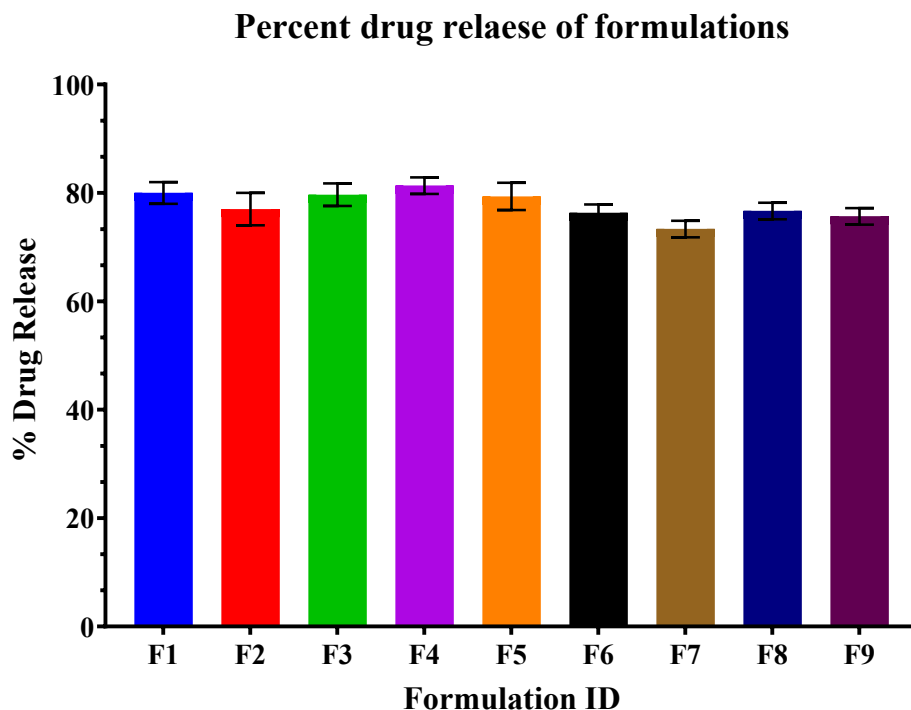


Figure 15. Comparative analysis of % drug release of mouth dissolving films formulations (F1-F9)  
 Table 17. Percent drug release of formulation F4 with respect to time

Time (min)	Formulation (F4)			MEAN <sup>[a]</sup>
	Experiment 1	Experiment 2	Experiment 3	
0.5	22	25	27	24.7 ± 2.52
1	28	30	32	30.0 ± 2.00
2	40	45	42	42.3 ± 2.52
3	50	55	48	51.0 ± 3.61
4	65	68	62	65.0 ± 3.00
5	70	74	69	71.0 ± 2.65
6	75	78	76	76.3 ± 1.53
7	80	82	81	81.0 ± 1.00

[a] Mean±SD of three different experiments

The highest release was found to be 81.0 ± 1.00 of the formulation. The F4 formulation showed better drug release as compare to other formulation.

### Zero order drug release plot of formulation F4

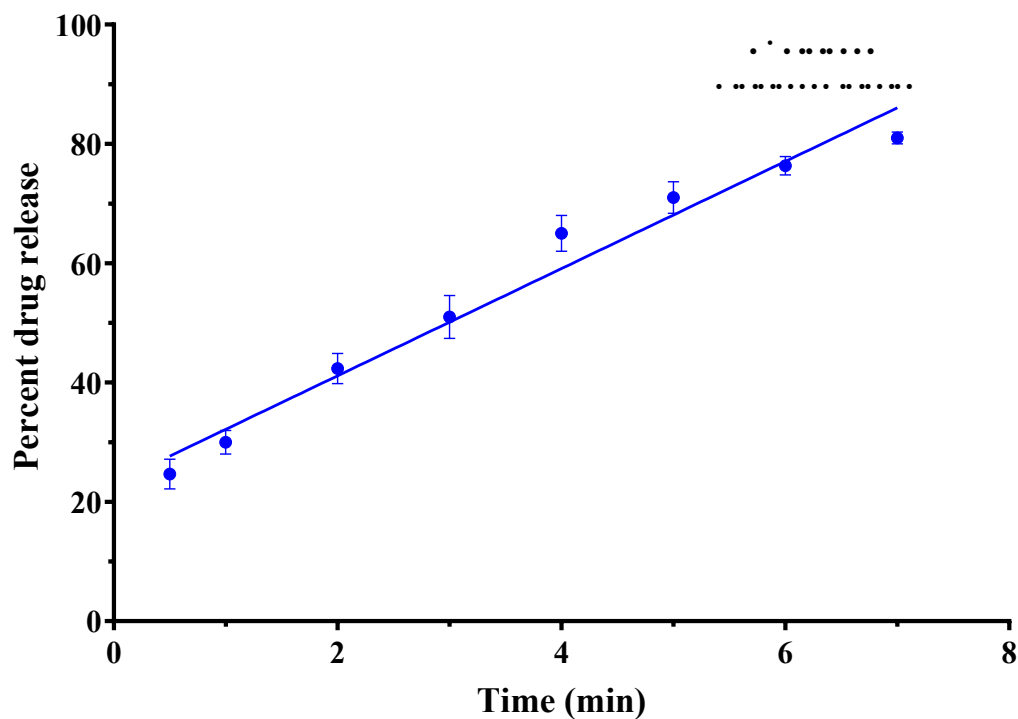


Figure 16. Graphical representation of Zero Order plot of formulation F4

### First order drug release plot of formulation F4

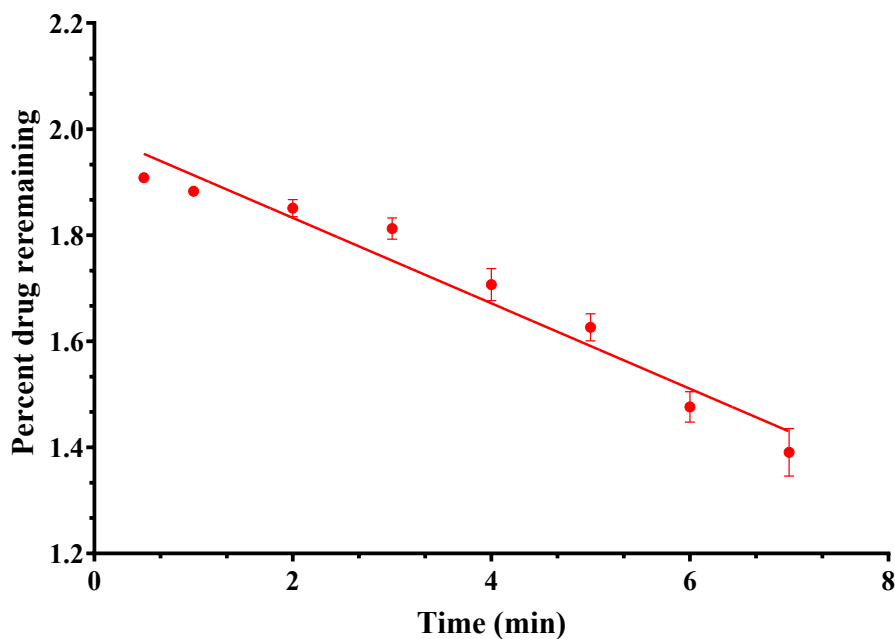


Figure 17. Graphical representation of first order plot of formulation F4

### Higuchi model for drug release of formulation F4

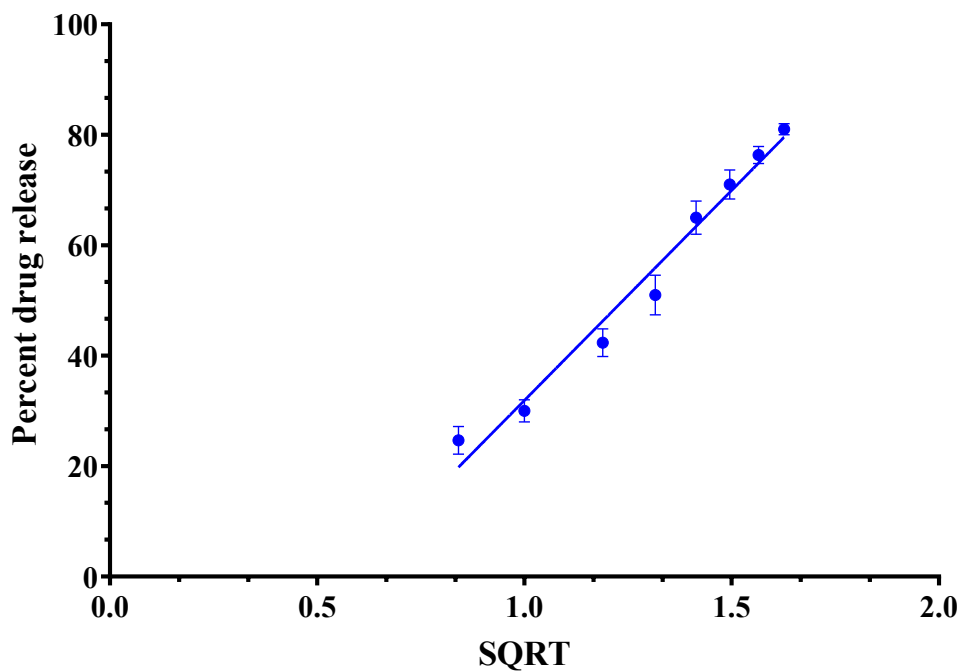


Figure 18. Graphical representation of Higuchi plot of formulation F4

### Korsmeyer Peppas model for release of formulation F4

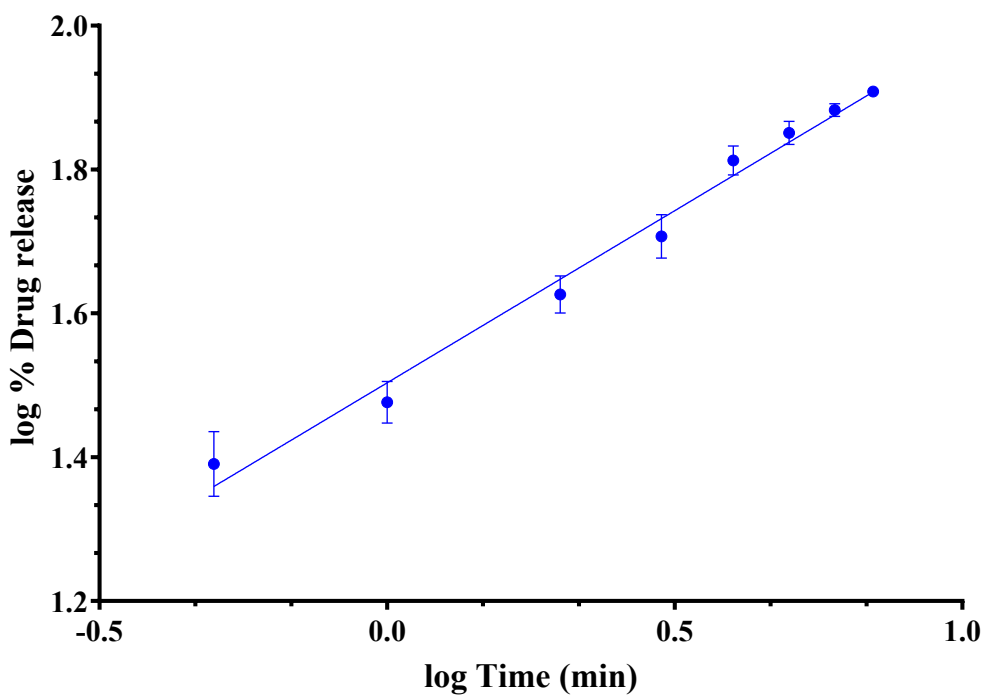


Figure 19. Graphical presentation of Korsmeyer-Peppas plot of formulation F4

**CONCLUSION**

The present research has demonstrated the successful development and comprehensive evaluation of mouth-dissolving films (MDF) of Artemether and Lumefantrine for the prevention and treatment of malaria. Employing the solvent casting method, a series of formulations were systematically optimized and subjected to rigorous assessment of key pharmaceutical parameters, including disintegration time, wetting time, percentage drug release, and folding endurance. Among the evaluated batches, the optimized film displayed a remarkably short disintegration time of  $47.33 \pm 0.47$  seconds and achieved a high dissolution rate of  $81 \pm 1.00$  %, indicating its capacity for rapid drug release in the oral cavity and swift therapeutic onset.

The mechanical and physicochemical characteristics of the films, such as uniform thickness, satisfactory folding endurance, and good handling properties, further reinforce their suitability for practical use and patient acceptability. The buccal delivery approach enables bypassing of first-pass hepatic metabolism, thereby improving systemic bioavailability of Artemether & Lumefantrine, and addressing the limitations associated with conventional solid dosage forms—especially in populations with swallowing difficulties or poor access to water.

Taken together, these findings highlight the potential of Artemether and Lumefantrine MDF as an advanced, patient-friendly alternative for malaria management, offering rapid onset of action, improved efficacy, and better treatment adherence. The developed formulation can not only enhance therapeutic outcomes but also contribute to the broader public health goal of malaria control by providing a robust, easy-to-administer delivery system for use in diverse healthcare settings.

**REFERENCE**

- Platon L, Lu F, Ménard D. World malaria report 2025: Growing biological threats, shrinking resources. *Decoding Infection and Transmission*. 2026;4. doi:10.1016/j.dcit.2026.100076
- Ariey F, Witkowski B, Amaratunga C, et al. A molecular marker of artemisinin-resistant *Plasmodium falciparum* malaria. *Nature*. 2014;505(7481):50-55. doi:10.1038/NATURE12876
- Conrad MD, Asua V, Garg S, et al. Evolution of Partial Resistance to Artemisinins in Malaria Parasites in Uganda. *N Engl J Med*. 2023;389(8):722-732. doi:10.1056/NEJMOA2211803
- Uwimana A, Legrand E, Stokes BH, et al. Emergence and clonal expansion of in vitro artemisinin-resistant *Plasmodium falciparum* kelch13 R561H mutant parasites in Rwanda. *Nature Medicine* 2020 26:10. 2020;26(10):1602-1608. doi:10.1038/s41591-020-1005-2
- Rosenthal PJ, Asua V, Conrad MD. Emergence, transmission dynamics and mechanisms of artemisinin partial resistance in malaria parasites in Africa. *Nat Rev Microbiol*. 2024;22(6):373-384. doi:10.1038/S41579-024-01008-2
- Rosenthal PJ, Asua V, Bailey JA, et al. The emergence of artemisinin partial resistance in Africa: how do we respond? *Lancet Infect Dis*. 2024;24(9):e591-e600. doi:10.1016/S1473-3099(24)00141-5
- Mihreteab S, Platon L, Berhane A, et al. Increasing Prevalence of Artemisinin-Resistant HRP2-Negative Malaria in Eritrea. *N Engl J Med*. 2023;389(13):1191-1202. doi:10.1056/NEJMOA2210956
- L'Episcopia M, Talha AA, Nour BYM, et al. High Prevalence of Artemisinin-Resistant *Plasmodium falciparum*, Southeastern Sudan. *Emerg Infect Dis*. 2025;31(6):1211-1215. doi:10.3201/EID3106.241810
- Visser JC, Woerdenbag HJ, Hanff LM, Frijlink HW. Personalized Medicine in Pediatrics: The Clinical Potential of Orodispersible Films. *AAPS PharmSciTech*. 2017;18(2):267-272. doi:10.1208/S12249-016-0515-1
- Scarpa M, Stegemann S, Hsiao WK, et al. Orodispersible films: Towards drug delivery in special populations. *Int J Pharm*. 2017;523(1):327-335. doi:10.1016/j.ijpharm.2017.03.018
- Borges AF, Silva C, Coelho JFJ, Simões S. Oral films: Current status and future perspectives II - Intellectual property, technologies and market needs. *J Control Release*. 2015;206:108-121. doi:10.1016/J.JCONREL.2015.03.012
- Ghosh TK., Pfister WR. Drug delivery to the oral cavity: molecules to market. Published online 2005:413. Accessed April 5, 2026. [https://books.google.com/books/about/Drug\\_Delivery\\_to\\_the\\_Oral\\_Cavity.html?id=RrxCEQAAQBAJ](https://books.google.com/books/about/Drug_Delivery_to_the_Oral_Cavity.html?id=RrxCEQAAQBAJ)
- Rushikesh Bhanage DG, DrAP, Bhanage R, Ghude D, Pawar DrA. Fast Dissolving Tablet: An Overview. *International Journal of Pharmaceutical Sciences*. 2025;03(05). doi:10.5281/ZENODO.15563036
- Ghosh TK., Pfister WR. Drug delivery to the oral cavity: molecules to market. Published online 2005:413. Accessed April 5, 2026. [https://books.google.com/books/about/Drug\\_Delivery\\_to\\_the\\_Oral\\_Cavity.html?id=RrxCEQAAQBAJ](https://books.google.com/books/about/Drug_Delivery_to_the_Oral_Cavity.html?id=RrxCEQAAQBAJ)
- Patel VF, Liu F, Brown MB. Advances in oral transmucosal drug delivery. ElsevierVF Patel, F

- Liu, MB Brown *Journal of controlled release*, 2011•Elsevier. 2011;153(2):106-116. doi:10.1016/J.JCONREL.2011.01.027
16. Pimple AP, Varsha Kudal MS, Sanap GS, Pooja Murkute MS, Professor A. A REVIEW: ROUTES OF DRUG ADMINISTRATION WITH THEIR RECENT ADVANCES. Published online 2022. Accessed April 5, 2026. www.ijcrt.org
17. Pareek V, Sci AKIJPP, 2014 undefined. Pharmaceutical packaging: current trends and future. researchgate.net V Pareek, A Khunteta Int J Pharm Pharm Sci, 2014•researchgate.net. Accessed April 5, 2026. https://www.researchgate.net/profile/Vikas-Pareek/publication/297091323\_Pharmaceutical\_packaging\_Current\_trends\_and\_future/links/59a696af4585156873cf9b3e/Pharmaceutical-packaging-Current-trends-and-future.pdf
18. Thoorens G, Krier F, Leclercq B, Carlin B, Evrard B. Microcrystalline cellulose, a direct compression binder in a quality by design environment—A review. Elsevier G Thoorens, F Krier, B Leclercq, B Carlin, B Evrard *International journal of pharmaceutics*, 2014•Elsevier. 2014;473(1-2):64-72. doi:10.1016/J.IJPHARM.2014.06.055
19. Rowe R, Sheskey P, Quinn M. Handbook of Pharmaceutical Excipients. 2006. Accessed April 5, 2026. https://ptacts.uspto.gov/ptacts/public-informations/petitions/1557270/download-documents?artifactId=oYmqeOY9z83KsyU4Bo609JAhS0tfEudMDCgS69tr77oGKwa8ROkdd28
20. Siciliano G, Alano P. Enlightening the malaria parasite life cycle: Bioluminescent Plasmodium in fundamental and applied research. *Front Microbiol.* 2015;6(MAY). doi:10.3389/FMICB.2015.00391/FULL
21. Organization WH. Management of severe malaria: a practical handbook. Вестник Росздравнадзора. 2012;4(1):9-15. Accessed April 5, 2026. https://iris.who.int/handle/10665/79317
22. Lindenberg M, Kopp S, Dressman JB. Classification of orally administered drugs on the World Health Organization Model list of Essential Medicines according to the biopharmaceutics classification system. Elsevier M Lindenberg, S Kopp, JB Dressman *European Journal of Pharmaceutics and Biopharmaceutics*, 2004•Elsevier. 2004;58(2):265-278. doi:10.1016/J.EJPB.2004.03.001
23. Journal ZPM, 2009 undefined. Coartem®: the journey to the clinic. Springer ZG Premji *Malaria Journal*, 2009•Springer. 2009;8(SUPPL. 1). doi:10.1186/1475-2875-8-S1-S3
24. Pethe AM, Desai RB. Formulation, optimization & evaluation of mouth dissolving film of nifedipine by using design of experiment. *Asian J Pharm Sci.* 2016;11(1):74-76. doi:10.1016/j.ajps.2015.10.059
25. Dinge A, Nagarsenker M. Formulation and evaluation of fast dissolving films for delivery of triclosan to the oral cavity. Springer A Dinge, M Nagarsenker *Aaps Pharmscitech*, 2008•Springer. 2008;9(2):349-356. doi:10.1208/S12249-008-9047-7
26. Charde YM, Avari JG. Bioavailability Enhancement of Artemether and Lumefantrine by Improving Solubility and Dissolution Rate using Solid Dispersion Technique. *Indian J Pharm Sci.* 2021;83(4):808-822. doi:10.36468/PHARMACEUTICAL-SCIENCES.832
27. El-Setouhy DA, El-Malak NSA. Formulation of a novel tianeptine sodium orodispersible film. Springer DA El-Setouhy, NSA El-Malak *Aaps Pharmscitech*, 2010•Springer. 2010;11(3):1018-1025. doi:10.1208/S12249-010-9464-2
28. Kumar GP, Phani AR, Prasad RGSV, et al. Polyvinylpyrrolidone oral films of enrofloxacin: Film characterization and drug release. Elsevier GP Kumar, AR Phani, R Prasad, JS Sanganal, N Manali, R Gupta, N Rashmi *International journal of pharmaceutics*, 2014•Elsevier. 2014;471(1-2):146-152. doi:10.1016/J.IJPHARM.2014.05.033
29. Yehia S, delivery OEGC drug, 2009 undefined. Fluconazole mucoadhesive buccal films: in vitro/in vivo performance. benthamdirect.com SA Yehia, ON El-Gazayerly, EB Basalious *Current drug delivery*, 2009•benthamdirect.com. 2009;6(1):17-27. doi:10.2174/156720109787048195
30. Mukherjee D, Research SBIS, 2013 undefined. Design and characterization of double layered mucoadhesive system containing bisphosphonate derivative. Wiley Online Library D Mukherjee, S Bharath *International Scholarly Research Notices*, 2013•Wiley Online Library. 2013;2013:1-10. doi:10.1155/2013/604690
31. Patel R, delivery SPC drug, 2009 undefined. Development and characterization of mucoadhesive buccal patches of salbutamol sulphate. ingentaconnect.com RS Patel, SS Poddar *Current drug delivery*, 2009•ingentaconnect.com. 2009;6(1):140-144. doi:10.2174/156720109787048177
32. Elmehad AN, El Hagrasy AS. Characterization and optimization of orodispersible mosapride

- film formulations. SpringerAN EIMeshad, AS El HagrasyAaps Pharmscitech, 2011•Springer. 2011;12(4):1384-1392. doi:10.1208/S12249-011-9713-Z
33. sankar ravisankar, <https://university.academia.edu/ravisankarsankar>. A review on analytical method development. Accessed April 5, 2026. [https://www.academia.edu/33538461/A\\_review\\_on\\_analytical\\_method\\_development](https://www.academia.edu/33538461/A_review_on_analytical_method_development)
34. Skoog, D.A., Holler, F.J. and Crouch, S.R. (2017) Principal of Instrumental Analysis. 7th Edition, Sunder College Publisher, New York. - References - Scientific Research Publishing. Accessed April 5, 2026. <https://www.scirp.org/reference/referencespapers?referenceid=2678907>
35. Satyanarayana DA, Keshavarao KP. Fast disintegrating films containing anastrozole as a dosage form for dysphagia patients. SpringerDA Satyanarayana, KP KeshavaraoArchives of pharmacal research, 2012•Springer. 2012;35(12):2171-2182. doi:10.1007/S12272-012-1215-3
36. Patra S, Sahoo R, Panda RK, Himasankar K, Barik BB. In vitro evaluation of domperidone mouth dissolving tablets. Indian J Pharm Sci. 2010;72(6):822-825. doi:10.4103/0250-474X.84607
37. Formulation and Evaluation of Mouth Dissolving Film of Ropinirole Hydrochloride by Using Pullulan Polymers. Accessed April 5, 2026. [www.ijpras.com](http://www.ijpras.com)
38. Mashru RC, Sutariya VB, Sankalia MG, Parikh PP. Development and evaluation of fast-dissolving film of salbutamol sulphate. Taylor & FrancisRC Mashru, VB Sutariya, MG Sankalia, PP ParikhDrug development and industrial pharmacy, 2005•Taylor & Francis. 2005;31(1):25-34. doi:10.1081/DDC-43947
39. Kumar SK, Nagabhushanam M, Rao KS, Bhikshapathi D. Preparation and in vivo evaluation of oral dissolving films containing sumatriptan succinate. Published online 2013.
40. Costa P, sciences JLE journal of pharmaceutical, 2001 undefined. Modeling and comparison of dissolution profiles. ElsevierP Costa, JMS LoboEuropean journal of pharmaceutical sciences, 2001•Elsevier. 2001;13(2):123-133. doi:10.1016/S0928-0987(01)00095-1